Emission Properties of Oxyluciferin and Its Derivatives in Water: Revealing the Nature of the Emissive Species in Firefly Bioluminescence

ARTICLE *in* THE JOURNAL OF PHYSICAL CHEMISTRY B · NOVEMBER 2014

Impact Factor: 3.3 · DOI: 10.1021/jp508905m · Source: PubMed

11 AUTHORS, INCLUDING:

Cyril Ruckebusch
Université des Sciences et Technologies de Li…
139 PUBLICATIONS **1,006** CITATIONS
SEE PROFILE

Eduard Fron
University of Leuven
63 PUBLICATIONS **796** CITATIONS
SEE PROFILE

Yves Mély
University of Strasbourg
326 PUBLICATIONS **7,298** CITATIONS
SEE PROFILE

Pance Naumov
New York University Abu Dhabi
162 PUBLICATIONS **1,910** CITATIONS
SEE PROFILE

THE JOURNAL OF PHYSICAL CHEMISTRY B

Article

Emission Properties of Oxyluciferin and its Derivatives in Water: Revealing the Nature of the Emissive Species in Firefly Bioluminescence

Avisek Ghose, Mateusz Rebarz, Oleg V. Maltsev, Lukas Hintermann, Cyril Ruckebusch, Eduard Fron, Johan Hofkens, Yves Mély, Pance Naumov, Michel Sliwa, and Pascal Didier

J. Phys. Chem. B, **Just Accepted Manuscript** • Publication Date (Web): 03 Nov 2014

Just Accepted

The Journal of Physical Chemistry B is published by the American Chemical Society. 1155 Sixteenth Street N.W., Washington, DC 20036

Emission Properties of Oxyluciferin and its Derivatives in Water: Revealing the Nature of the Emissive Species in Firefly Bioluminescence

Avisek Ghose,[†,¶] Mateusz Rebarz,[‡,¶] Oleg V. Maltsev,[§] Lukas Hintermann,[§] Cyril Ruckebusch,[‡] Eduard Fron,[‖] Johan Hofkens,[‖] Yves Mély,[†] Panče Naumov,[*,#] Michel Sliwa,[*,‡] Pascal Didier,[*,†]

[†]*Laboratoire de Biophotonique et Pharmacologie, UMR 7213 du CNRS, Faculté de Pharmacie, Université de Strasbourg, 74, Route du Rhin, 67401 Illkirch Cedex, France*
[‡]*Laboratoire de Spectrochimie Infrarouge et Raman (LASIR), CNRS UMR 8516/Université Lille Nord de France, Université Lille1 – Sciences et Technologies/Chemistry Department, bât C5/59655 Villeneuve d'Ascq Cedex, France*
[§]*Department Chemie, Technische Universität München, Lichtenbergstr. 4, 85748 Garching bei München, Germany*
[‖]*Laboratory of Photochemistry and Spectroscopy, Department of Chemistry, KU Leuven, Celestijnenlaan 200F, 3001 Heverlee, Belgium*
[#]*New York University Abu Dhabi, PO Box 129188, Abu Dhabi, United Arab Emirates*

Abstract

The first systematic steady-state and time-resolved emission study of firefly oxyluciferin (emitter in firefly bioluminescence) and its analogues in aqueous buffers provided the individual emission spectra of all chemical forms of the emitter and the excited-state equilibrium constants in strongly polar environment with strong hydrogen bonding potential. The results confirmed the earlier hypothesis that excited-state proton transfer from the enol group is favored over proton transfer from the phenol group. In water, the phenol-keto form is the strongest photoacid among the isomers and its conjugate base (phenolate-keto) has the lowest emission energy (634 nm). Furthermore, for the first time we observed green emission (525 nm) from a neutral phenol-keto isomer constrained to the keto form by cyclopropyl substitution. The order of emission energies indicates that in aqueous solution a second deprotonation at the phenol group after the enol group had dissociated (that is, deprotonation of the phenol-enolate) does not occur in the first excited state. The pH-dependent emission spectra and the time-resolved fluorescence parameters revealed that the keto-enol tautomerism reaction, which can occur in a non-polar environment (toluene) in the presence of a base, is not favored in water.

Keywords: ESPT, time resolved spectroscopy, fluorescence, photoacid, chemometrics

1.Introduction

1.1.Background

The phenomenon of bio-chemiluminescence (commonly known as bioluminescence) is a fascinating natural process by which living organisms convert chemical energy into light. Such cold-light emission from a chemically produced excited (chemiexcited) state is known for several organisms, including certain species of bacteria, beetles, squid, and worms.[1-3] In the case of fireflies, the light-generating reaction involves an enzyme (luciferase) that catalyzes oxidation of the substrate (luciferin) by molecular oxygen, in the presence of adenosine-5′-triphosphate (ATP) and Mg^{2+}, leading to formation of the emitting molecule (oxyluciferin, **$OxyLH_2$**) in its first excited state.[2, 4-5] While relaxing to its ground state, **$OxyLH_2$** emits a photon in the visible part of the electromagnetic spectrum. The high luminescence quantum yield of this process[6] reflects not only a very efficient catalytic machinery, but also highly favorable micro-environment with strongly deactivated non-radiative pathways. With its high quantum yield[6] and the exceptionally high signal-to-noise ratio due to the absence of photo-excitation, the firefly bioluminescence stands out as the best candidate of choice for bioimaging applications.[7-12]

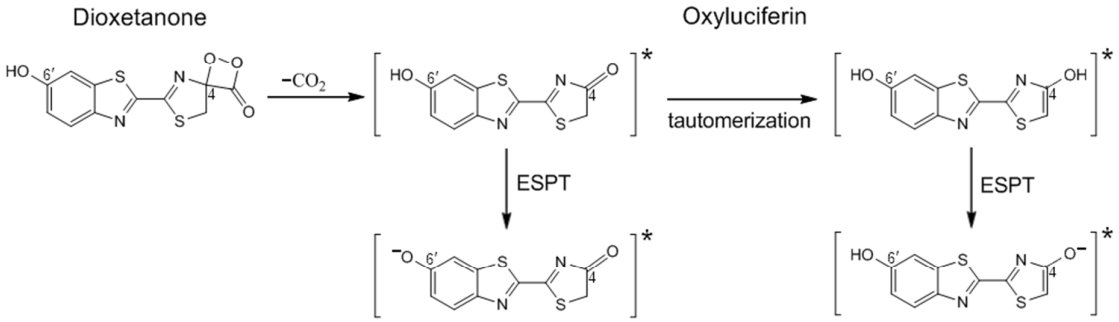

Scheme 1. Thermal decomposition of dioxetanone (unstable intermediate) to chemiexcited firefly oxyluciferin and possible deexcitation pathways of the emitter.

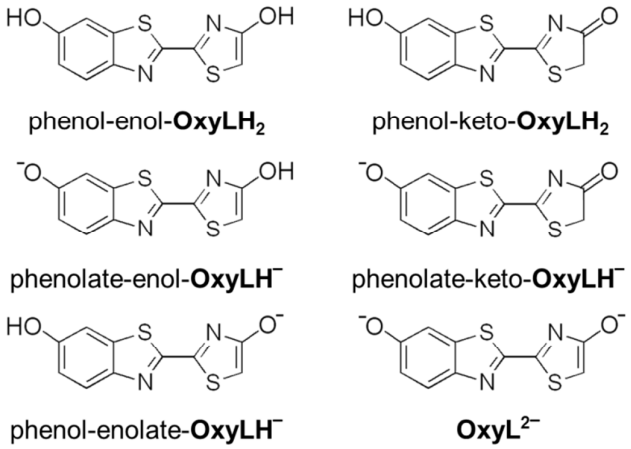

Chart 1. Possible ground-state chemical forms of firefly oxyluciferin in solution.

The reaction chemistry and structure of the emitter are identical for all known beetle luciferases,[1, 13] however the emission wavelength depends on the conditions and can vary between 536 nm and 638 nm.[14] Despite being essential to the development of new bioanalytical tools, the chemical origin of the color modulation remains poorly understood. According to several debated photophysical mechanisms, the color modulation likely occurs as a result of intramolecular and/or intermolecular factors within the enzyme.[15] The emitter is generated by decomposition of the dioxetanone and release of CO_2 (Scheme 1). Because isolation of this highly unstable species has not been achieved yet, most spectroscopic studies were performed by photoexcitating either **OxyLH$_2$** alone or its complex with the enzyme in solution.[16]

Even though the complex chemistry of **OxyLH$_2$** has spurred extensive experimental[3, 6, 16-27] and theoretical[28-40] studies, the photophysics of this 'phantom molecule' remains poorly characterized. It can exist in six different forms as a result of ionization of two hydroxyl groups and the keto-enol tautomerism of the 4-thiazolone subunit (Chart 1). The intricate triple dynamic chemical equilibrium in solution is strongly affected by the solvent, pH, and specific interactions with bases.[41-44] Moreover, the spectral properties of each chemical form could be additionally affected in the enzyme by the nature of the active site such as polarity, presence of additional ions, and π–π stacking.[42, 45-46] Historically, the phenolate-keto species has been considered the most viable form for the emitting state.[17, 35, 40] However, recent studies have shown that the enol tautomer should not be excluded as emitting species that is generated in the excited state.[42, 47-48] Moreover, ultrafast spectroscopic results have indicated possible excited-state proton transfer (ESPT) from either of the two hydroxyl groups (Scheme 1).[47, 49] Experimental[50] and theoretical[51] studies of the firefly luciferin (the reaction precursor) have shown that the photoluminescence pathways of this closely related molecule also depend strongly on pH and excitation wavelength.

One of the obstacles to complete understanding of the deexcitation processes is the limited information on the excited-state dynamics of the emitter in aqueous solutions. To determine the accurate ground-state equilibrium constants of **OxyLH$_2$**, we have recently applied the multivariate curve resolution–alternating least squares (MCR-ALS) procedure and deciphered the pH-dependent spectra of model compounds where some ESPT processes or the enol-keto equilibrium are blocked.[43] The analysis provided for the first time the absorption spectra and the pH-dependent concentration profiles of the individual chemical forms of the emitter devoid from the other species.. Encouraged by this result, here we apply a similar approach to investigate the *emission* spectra and equilibrium constants in the excited state for all chemical forms of **OxyLH$_2$**. These parameters have not been determined, even that they are essential for clarification of the related photophysics. We prepared five analogues of firefly oxyluciferin, including two new structural variants, 5,5-**Cpr-OxyLH** (Cpr = (spiro)cyclopropyl) and 6′-**Me-5,5-Cpr-OxyL** (Chart 2).[52] The latter two compounds were used instead of the 5,5-dimethyl analogue (5,5-**DMeOxyLH**), which in our hands proved to be unstable under photoexcitation. The steady-state and time-resolved emission experiments, performed in aqueous buffered solutions within a physiologically relevant pH range, provided for the first time the individual emission spectra of all tautomeric and anionic variants of **OxyLH$_2$** as well as the equilibrium constants in the excited state. In addition, the rate constants of the fundamental photoreaction processes were also determined.

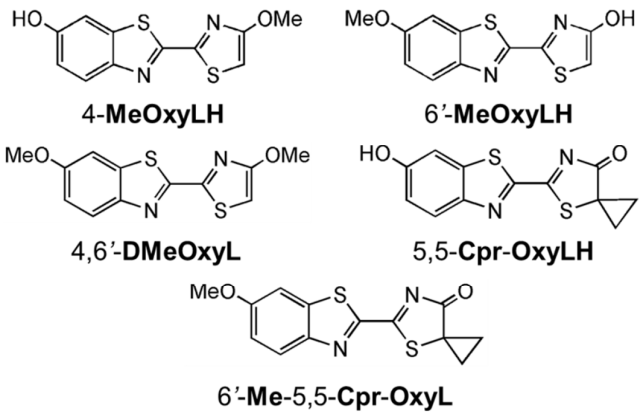

Chart 2. Derivatives of firefly oxyluciferin studied in this work.

2. Experimental section

2.1. Sample preparation. The synthesis of **OxyLH$_2$** was performed by our improved procedure.[44] The model analogues 4-**MeOxyLH**, 6′-**MeOxyLH** and 4,6′-**DMeOxyL** were synthesized as previously reported.[43] The synthesis and characterization of the new spirocyclic analogues 5,5-**Cpr-OxyLH** and 6′-**Me**-5,5-**Cpr-OxyL** will be reported elsewhere. Stock solutions of all compounds were prepared in spectroscopic grade DMSO (Sigma-Aldrich) and stored in several aliquots at –20 °C to minimize the freeze-thaw cycle. They were further diluted thousand-fold to a final concentration of about few micromolar in aqueous buffer with different pH. The buffers were prepared by diluting a 1 M stock solution in deionized, Millipore-purified water (18.2 MΩ). Buffered stock solutions were prepared as follows: 75 mM NaCl/20 mM KH_2PO_4/0.2 mM $MgCl_2$ for pH ≤ 7.0 and 75 mM NaCl/25 mM Tris(hydroxymethyl)amenomethane (TRIS)/0.2 mM $MgCl_2$ for pH > 7.0. The buffer was separated into several fractions and their pH (error ±0.02) was adjusted by 250 mM HCl or by 250 mM NaOH separately at 20 °C (ΔpH ≈ 0.25). Separate buffers at different pH were used in all spectral measurements.

2.2. Spectroscopy. Absorption spectra were recorded with a Cary-4000 spectrometer (Agilent Technologies). Steady-state fluorescence spectra were recorded with Fluorolog 3 spectrofluorometer (Horiba Jobin Yvon) with 3-nm excitation/emission slit and corrected for the instrumental response characteristics. The absolute quantum yield determined for three selected compounds in phosphate buffered solution (Bio Whittaker) at pH 7.4 and 20 °C was 0.49 ± 0.05 for 4,6′-**DMeOxyL**, 0.65 ± 0.07 for 4-**MeOxyLH** and 0.19 ± 0.02 for 5,5-**Cpr-OxyLH**. These compounds were selected as references because they exhibit distinct emission band centered at 445, 560 and 637 nm, respectively. The fluorescence quantum yields of the other compounds were determined by the comparative method, using the equation $\Phi_S = \Phi_R*(I_S/I_R)*(OD_R/OD_S)*(n_S^2/n_R^2)$.[53]

The fluorescence decays of all compounds were measured by the Time-Correlated Single Photon Counting (TCSPC) technique. Excitation pulse was provided by a femtosecond Ti:Sapphire laser (Coherent Chameleon Ultra II, 80 MHz, 200 fs, 3.8 W) coupled to either a pulse picker (4 MHz) and a harmonic generator (SHG/THG, APE) for excitation from 300 to 500 nm, or an intracavity frequency doubled OPO (APE) and a pulse picker (4 MHz) for 500 to 700 nm excitation. The measurements of fluorescence lifetimes were performed using the

FT200 Picoquant spectrometer. The emission was collected through a polarizer set at the magic angle and Czerny-Turner type monochromator computer controlled for the selection of wavelength detection. The single-photon events were collected by a cooled microchannel plate photomultiplier tube R3809U (Hamamatsu) and recorded by a PicoHarp 300 TCSPC system (PicoQuant). The instrumental response function was recorded using colloidal silica (Ludox) and its full width at half-maximum was ~50 ps. All decays were collected until the number of events reached 10^4 at the maximum. The recorded decays were analyzed by the FluoFit software package ver. 4.6.6 (PicoQuant). The reduced χ^2 was below 1.1. Weighted residuals and autocorrelation function were used to check the quality of the fits. In case of non-exponential decays the stretched exponential model was used to estimate the time constants.

3. Results and Discussion

3.1. Selection of model compounds and their pH-dependent absorption spectra

The photochemistry of **OxyLH$_2$** in aqueous solution is quite complex because of its triple equilibrium (ionization of both hydroxyl groups and keto-enol tautomerization of the thiazole moiety). Similar to the strategy of selective blocking of either hydroxyl group employed earlier,[42-43, 54] we chose to study five compounds that model different tautomeric and anionic variants of **OxyLH$_2$** (Chart 2). Specifically, 4,6′-**DMeOxyL** is a model for the phenol-enol-**OxyLH$_2$** form, whereas 4-**MeOxyLH** and 6′-**MeOxyLH** are analogous to the phenolate-enol-**OxyLH$^-$** and phenol-enolate-**OxyLH$^-$** forms that are normally generated in basic conditions. We also included in the analysis two derivatives in which the 5,5-disubstitution pattern restricts the thiazole portion to the keto tautomeric form; 5,5-**Cpr-OxyLH**, whose phenol group is deprotonated in basic media, mimics the phenolate-keto-**OxyLH$^-$** form, while 6′-**Me**-5,5-**Cpr-OxyLH** is a model for the neutral phenol-keto-**OxyLH$_2$** form. Notably, previous studies have relied on the doubly methylated analogue, 5,5-**DMeOxyLH**, to model the keto form.[45, 54-55] However, our experiments indicated that this compound is not stable and in fact, very photo-unstable (an important parameter for our studies) in aqueous solutions, especially in basic condition and under UV excitation. Instead, we used cyclopropyl derivatives, 5,5-Cpr-**OxyLH** and 6′-Me-5,5-Cpr-**OxyL** (Chart 2), which exhibit significantly better stability and photostability, as it was concluded from the comparison of pH-dependent absorption and emission spectra between 5,5-Cpr-**OxyLH** and 5,5-**DMeOxyLH** (see Fig. S1 in the Supporting Information, SI). For 5,5-**DMeOxyLH** and 5,5-Cpr-**OxyLH** in basic condition and under UV excitation, a new photoproduct with emission band at 530 nm is formed which is assigned to dianionic species (see section 3.4) that evolves after isomerization and hydrolysis. The cyclopropyl group minimized such photoreaction and increased the global stability in the ground state and in the excited state. A minor influence of cyclopropyl group can be observed on the absorption spectrum (Fig. 1b and Fig. 1d, SI Fig. S1): the existence of a shoulder about 370 nm which does not exist for 5,5-**DMe-OxyLH**. This shoulder is assigned to a certain geometry constrained by the cyclopropyl group on the thiazole ring. Indeed theoretical calculations predict that the lowest excitation for 5,5-**DMe-OxyLH** as well as phenol-keto-**OxyLH$_2$** is a charge transfer transition (HOMO-LUMO) from phenol part to thiazole ring and that the geometry of the thiazole ring is nearly planar[37,45] without cyclopropyl group.

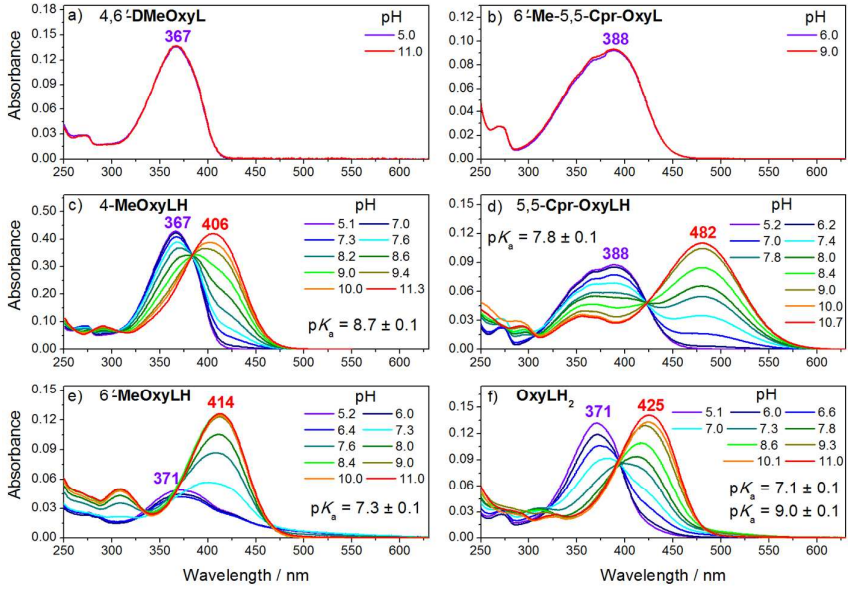

Figure 1. Dependence of the absorption spectra of firefly oxyluciferin (**OxyLH$_2$**) and its derivatives in aqueous solutions at different pH and determination of the corresponding pK_a values. The structural formulas are given in Chart 2. The spectra were recorded in aqueous buffers at different pH (see section 2.1) at 20 ^{o}C. The concentration was 0.9, 6.0, 4.0, 1.0, 1.1 and 3.0 μM for 4,6′-**DMeOxyL**, 4-**MeOxyLH**, 6′-**MeOxyLH**, 6′-**Me**-5,5-**Cpr**-**OxyL**, 5,5-**Cpr**-**OxyLH** and **OxyLH$_2$**, respectively.

The interpretation of the emission spectra required characterization of the composition, concentration, and absorbance spectra of **OxyLH$_2$** and its derivatives in the pH range 5–11. The pH-dependent steady-state absorption spectra are presented in Fig. 1. The molecules that are constrained to only two chemical forms (5,5-**Cpr**-**OxyLH** and 4-**MeOxyLH**) present clear isosbestic points. The spectrum of 5,5-**Cpr**-**OxyLH** (Fig, 1d) indicates that the spectral maximum of the phenolate ion of the keto form is strongly red shifted (482 nm) relative to the neutral form (388 nm). The pK_a = 7.8 is identical to and confirms the value previously determined for 5,5-**DMeOxyLH**.[43]

However, extraction of the pure spectra of the species that evolve from 6′-**MeOxyLH** and **OxyLH$_2$** was not straightforward and required a multiset-data analysis of the pH-dependent absorption spectra of **OxyLH$_2$** and its derivatives. Following the previously described approach,[43] we used here different buffers (see the experimental section) together with the new cyclopropyl derivatives to evaluate eventual effects of the buffer on the spectra. Application of such analysis (SI Fig. S2) afforded the pH-dependent concentration profiles and the absorption spectra of the individual chemical forms at various pH (Fig. 2). In line with earlier results,[43] the spectral maxima of the chemical forms are aligned in the following order (Fig. 6 and Fig. S2, SI): phenol-enol-**OxyLH$_2$** (367 nm) < phenol-keto-**OxyLH$_2$** (388 nm) < phenolate-enol-**OxyLH$^-$** (406 nm) < phenol-enolate-**OxyLH$^-$** (414 nm) < **OxyL^{2-}** (425 nm) < phenolate-keto-**OxyLH$^-$** (482 nm). The distribution diagram (Fig. 2) shows that the contribution of the phenolate-enol-**OxyLH$^-$** form is negligible due to the significantly higher pK_a value of the phenol (pK_a = 9.0) relative to the enol (pK_a = 7.1) group. In practice, the presence of this species in solutions of **OxyLH$_2$** can be ignored.

The pK_a values determined in TRIS buffer are slightly lower than those in phosphate buffer.[43] In particular, the phenol-phenolate equilibrium for 4-**MeOxyLH** is lower by 0.2 pK units, whereas the pK_a constants for **OxyLH$_2$** are lowered by 0.3 units for the phenol-enol/phenol-enolate and 0.1 units for the phenol-enolate/phenolate-enolate equilibrium, respectively. Apparently, the chemical equilibria of **OxyLH$_2$** and its derivatives are slightly sensitive to the ionic strength of the buffer. Finally, the combination of the concentration profiles and absorption spectra allows us to determine the absorption contribution of each individual component at a given pH value (Fig. 2). In turn, it is possible to select precisely the excitation wavelength to preferentially excite a particular chemical form of the emitter. For instance, at pH 8–9 (Fig, 2d and 2e) it is possible to selectively excite the phenolate-keto-**OxyLH$^-$** form (SI Fig. S7) and to study its photodynamics without significant contribution from the other forms.

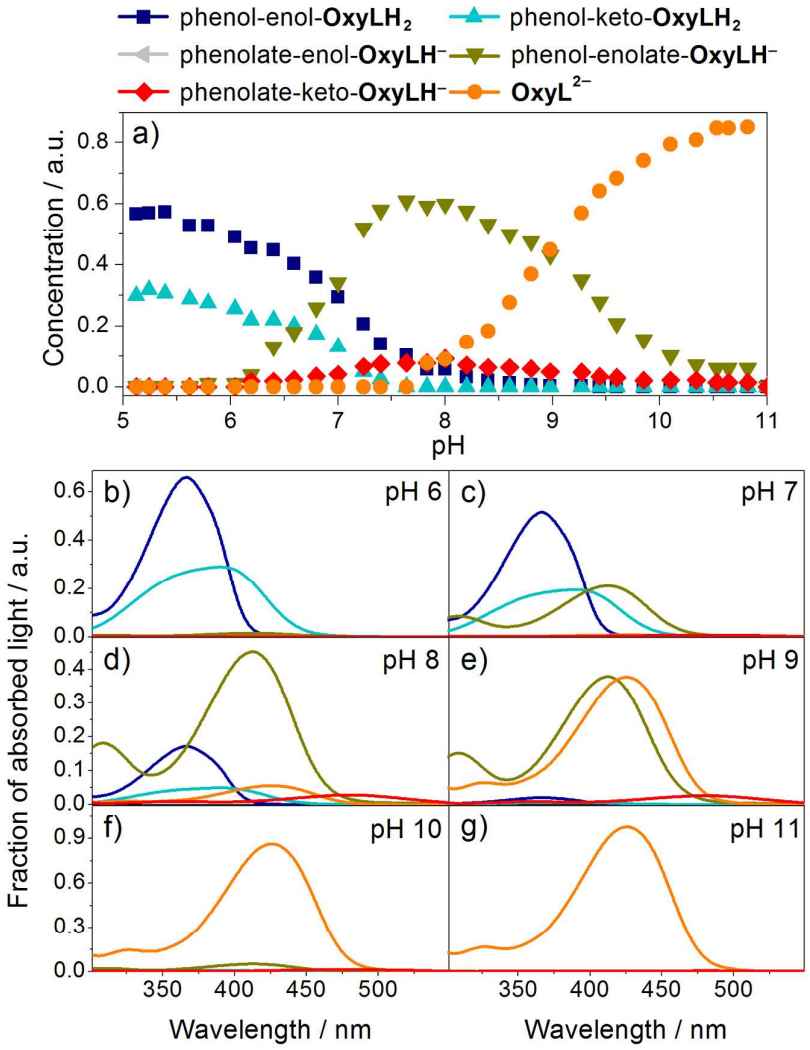

Figure 2. Absorption spectra and pH-concentration profiles of five forms of firefly oxyluciferin obtained by MCR-ALS analysis. The concentration of the phenolate-enol-**OxyLH$^-$** form under these conditions is negligible.

The ground-state equilibria and the absorption spectra of the conjugated acids and bases set the basis for the estimation of the corresponding equilibrium constants in the excited state (pK_a*) by means of the Förster cycle.[53, 56] Although this method can only provide qualitative estimate, it can be used for assignment of the emissive species in the excited state (vide infra). With an estimated pK_a* = –2.6, the most photoacidic of the studied compounds is 5,5-**Cpr-OxyLH**. This value places this derivative in the group of "super-photoacids" (pK* < 0) which undergo deprotonation even in alcohols and some other organic solvents.[57] On the other hand, 4-**MeOxyLH** has a much higher pK_a* value, estimated to 3.4. The comparison of these values shows that the photoacidity of the phenol group is strongly affected by the keto-enol tautomerism on the opposite terminus of the emitter. A similar effect was observed for the acidity in the ground state. For the enol-enolate equilibrium in 6′-**MeOxyLH**, we estimate a pK_a* value of 1.7.

In the case of **OxyLH$_2$***, five equilibria should be considered: phenol-enol/phenol-enolate, phenol-enolate/phenolate-enolate, phenol-enol/phenolate-enol, phenolate-enol/phenolate-enolate and phenol-keto/phenolate-keto. In the ground state, where the enol group is more acidic than the phenol group (pK_a = 7.1 vs pK_a = 9.0), the pathway including phenol-enol/phenolate-enol deprotonation (this is confirmed in the section 3.4 that the phenol group has a lower photo-acidity than the enol one in phenol-enol form, Table 2) and subsequent phenolate-enol/phenolate-enolate deprotonation can be excluded from consideration. Moreover, the equilibrium phenol-enolate/phenolate-enolate is accompanied with a minor difference between the respective absorption spectra, which gives a pK_a* of 7.5 and implies absence of ESPT in acidic and neutral conditions. The deprotonation of the enol group gives estimated pK_a* = 1.5 for the phenol-enol/phenol-enolate equilibrium (note that this value is higher than the previously reported values, between –0.5 and 0.5[49, 58] and should be corrected with the emission spectra, see section 3.4). For the phenol-keto/phenolate-keto equilibrium, the calculated constant is identical to that obtained for 5,5-**Cpr-OxyLH** (pK_a* = –2.6), indicating that only anionic species will be observed after photoexcitation.

3.2. Emission spectra of the non-ionizable model compounds

The fluorescence spectra of 4,6′-**DMeOxyL** and 6′-**Me**-5,5-**Cpr-OxyL** recorded in buffered aqueous solutions are presented in Fig. 3a and 3b, and the corresponding fluorescence decays are deposited as SI Fig. S3. As expected from the absence of acidic groups, the position and shape of their spectra as well as the total fluorescence quantum yield and fluorescence lifetimes do not evolve with pH in the studied range (Fig. 3, Table 1). 4,6′-**DMeOxyL** exhibits a single broad band with a maximum at 445 nm, in good agreement with the emission assigned to the neutral phenol-enol-**OxyLH$_2$** form (450–455 nm).[54, 58] The fluorescence quantum yield of this compound was 49% and the emission decayed monoexponentially with a lifetime of 3.1 ns. On the other hand, the emission maximum of 6′-**Me**-5,5-**Cpr-OxyL**, an analogue of the phenol-keto-**OxyLH$_2$** form, was significantly redshifted from that of the phenol-enol-**OxyLH$_2$** model (4,6′-**DMeOxyL**) counterpart, with a maximum at 525 nm and monoexponential decay with a time constant of 0.9 ns. This lifetime shortening could be attributed to increased contribution from non-radiative pathways due to the smaller energy gap.

The position of the emission maximum of 6′-**Me**-5,5-**Cpr-OxyL** is noteworthy because phenol-keto-**OxyLH$_2$** has so far been regularly reported as blue emitter.[42, 55, 58] That assignment was based mainly on results obtained for the model compound 5,5-**DMeOxyLH** in organic solvents. Due to the very high photoacidity of this compound (pK* = –3.91)[55] the

emission of its neutral form cannot be recorded in water, even in quite acidic solution, and only the spectrum of the phenolate anion is observed. The deprotonation is inhibited in many organic solvents, such as benzene, chloroform and acetonitrile. However, Hirano et al. showed that the emission of 5,5-**DMeOxyLH** depends on polarity.[45] Hence, the results obtained in organic solvents cannot be merely extrapolated to very polar solution (water). The same authors provided insight into the emission of the keto-**OxyLH$_2$** form in water by blocking the ionization of the 6′-OH group by methylation of 5,5-**DMeOxyLH.** However, the product (6′-**Me-5,5-DMeOxyL**) was unstable and the emission could only be estimated as green light (~535 nm). In contrast, the derivative studied here 6′-**Me**-5,5-**Cpr**-**OxyL** is stable in water within the pH range 5–9, and its green emission could be recorded without difficulties. This result indicates that the phenol-keto-**OxyLH$_2$** form, normally identified in non-aqueous solutions as blue emitter, could emit green light in very polar and strong hydrogen acceptor solvent such as water. However, similar to the case of 6′-**Me-5,5-DMeOxyL**[45] the electronic effects could not be excluded[42] as possible reason for the observed shift.

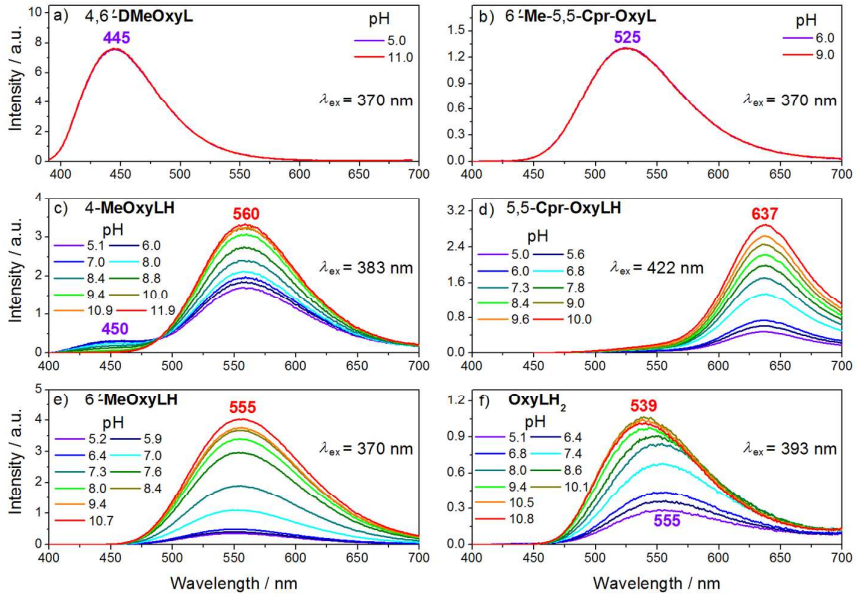

Figure 3. Emission spectra of firefly oxyluciferin (**OxyLH$_2$**) and its derivatives recorded in aqueous solutions at different pH. The chemical formulas are given in Chart 2. Measurements were performed at room temperature (20 °C) in aqueous buffers at different pH (see section 2.1) and the concentration was 0.9, 6, 4, 1, 1.1 and 3 μM for 4,6′-**DMeOxyL**, 4-**MeOxyLH**, 6′-**MeOxyLH**, 6′-**Me**-5,5-**Cpr**-**OxyL**, 5,5-**Cpr**-**OxyLH** and **OxyLH$_2$**, respectively.

3.3. Emission spectra of the ionizable model compounds

The fluorescence spectra of 4-**MeOxyLH**, 5,5-**Cpr**-**OxyLH** and 6′-**MeOxyLH** recorded in aqueous solutions within the pH range 5–11 are presented in Fig. 3. The spectra of 4-**MeOxyLH** and 5,5-**Cpr**-**OxyLH** were recorded at an excitation wavelength that corresponds to the isosbestic points of 383 nm and 422 nm (Fig. 1a and 1b). 5,5-**Cpr**-**OxyLH** was always irradiated in the visible region. Excitation to higher excited states leads to formation of a new photo-product which has a characteristic specific emission at 530 nm, which was particularly

pronounced in basic conditions for UV excitation (SI Fig. S1). 6′-**MeOxyLH** was excited at 370 nm where the absorption was least sensitive to pH.

The spectra of 4-**MeOxyLH** in acidic solutions are composed of two bands (Fig 3c). At the lowest studied pH (5) the strong band centered at 560 nm from the ion is accompanied by a weaker band at ~450 nm from the neutral form, in accordance with the spectrum of 4,6′-**DMeOxyL**. This assignment is supported by the time-resolved fluorescence decays recorded in acidic solution (pH 5). As shown in Fig. 4a, by excitation of the neutral form (absorption at 370 nm) the emission band at 450 nm is strongly quenched and decays non-exponentially. Simultaneously the fluorescence band at 560 nm rises (Fig. 4a) with an average time constant corresponding to proton transfer rate and disappears biexponentially with lifetimes 1.5 and 4.9 ns (Fig. 4, Table 1), where the first component corresponds to geminate proton quenching (SI Fig. S6). In agreement with a pK_a* value of about 3.4 (see section 3.1), the 450 nm band completely vanishes in basic solution where only the deprotonated excited state contributes to the emission (Fig. 3c). At pH 10, the deprotonation occurs already in the ground state so that growing of the luminescence and, expectedly, geminate recombination was not observed. The emission at 560 nm was thus characterized by a monoexponential decay with a time constant identical to that of the longer component (4.9 ns) measured at pH 5 (Table 1). Thus, the spectrum recorded at high pH establishes a viable model for the fluorescence signature of the phenolate-enol-**OxyLH**$^-$ form.

To obtain the spectral signature of the phenolate-keto-**OxyLH**$^-$ form, we examined the spectra of 5,5-**Cpr-OxyLH**. In contrast to 4-**MeOxyLH,** the shape and position of the spectra did not evolve with pH and only one band with a maximum at 637 nm was observed (Fig. 3d). This result can be explained by the much higher photoacidity of this compound which undergoes very efficient ESPT throughout the whole pH range studied here. The fluorescence decay recorded at 520 nm, corresponding to the neutral form keto-**OxyLH$_2$**, reveals a bimodal process (Fig. 4d) with the short component corresponding to the instrumental response function (IRF) of the setup (< 50 ps). Thus, ESPT from the phenol group is a very fast process, and only emission from the deprotonated form of the molecule could be observed with steady-state spectroscopy. The maximum at 637 nm is in very good agreement with the data reported previously for the phenolate-keto emission based on the 5,5-**DMeOxyLH** derivative.[45, 55] It is worthy of note that deexcitation of the phenolate-keto anion exhibits a time constant τ = 0.6 ns and is several times faster than for the corresponding phenolate-enol form (τ = 4.9 ns; compare with the data in Fig. 4a and Table 1). As mentioned above, the weak emission and the long tail at 530 nm at basic pH are due to photo-degradation and should not be taken into account when the spectra of the phenolate-keto form are considered.

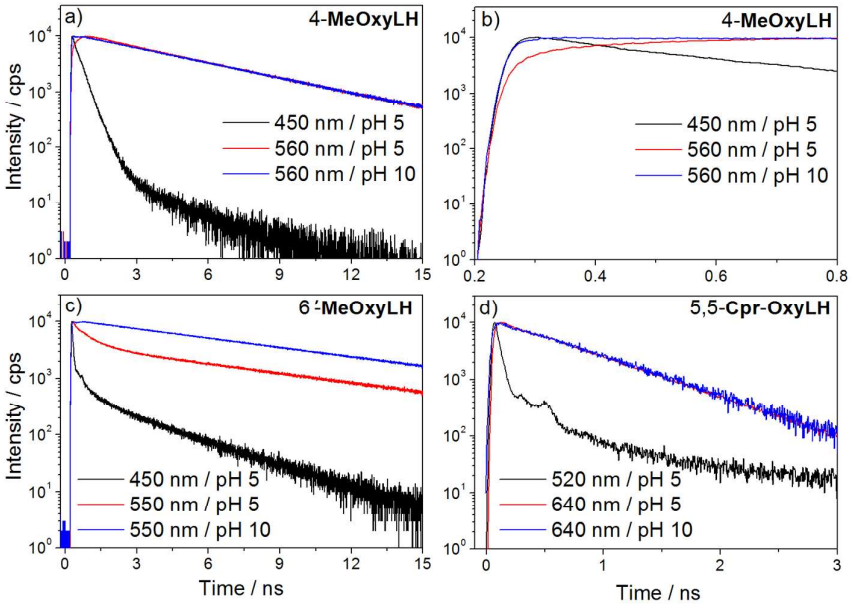

Figure 4. Fluorescence decays of derivatives of firefly oxyluciferin measured in acidic and basic buffered aqueous solutions. The chemical formulas are given in Chart 2.

To obtain insight into the emission properties of phenol-enolate-**OxyLH**$^-$, we turned to 6′-**MeOxyLH**, where the dissociation of the phenol group is blocked. This derivative exhibits a broad intense emission at ~550 nm (Fig. 3e). The strong photoacidity that was qualitatively evaluated above indicates that in the studied pH range the emission of 6′-**MeOxyLH** originates mainly from the enolate ion. Indeed, the fluorescence decay recorded at 450 nm has a non-exponential character with IRF signature at short timescale (Fig. 4c), confirming the very fast and efficient ESPT from the enol group. However, it is already known from the absorption spectra[43] that this compound can exist as a mixture with ~30% keto form at pH = 5. In consequence, the contribution of this tautomer (exclusively in the neutral form due to blocked phenol deprotonation) to the emission spectra of 6′-**MeOxyLH** cannot be precluded, especially at acidic pHs. Indeed, thorough analysis of the pH-dependent spectra (Fig. 3e) reveals small blue shift of the spectrum from 555 nm at pH 11 to 550 nm at pH 5. This energy change could be explained by superposition of two broad and strongly overlapping components in the spectrum recorded in acidic medium: a minor component that corresponds to the neutral keto tautomer that emits at ~525 nm (compare with 6′-**Me**-5,5-**Cpr-OxyL**) and a major component that originates from the enolate anion, with a maximum at 555 nm. At higher pH the first species is depleted and at basic pH only emission from the pure enolate form could be observed.

To support this interpretation, we recorded the emission spectrum of 6′-**MeOxyLH** at pH 5 after excitation at 430 nm (SI Fig. S4). Under these conditions, the excitation of the keto tautomer is strongly favored because of the superior absorption coefficient relative to the other species.[43] Its contribution to the emission in the resultant spectrum was more pronounced and the blue shift of the maximum towards 535 nm became more apparent. Moreover, the presence of the keto tautomer was also manifested in the time-resolved fluorescence. The decay recorded in acidic solution at 550 nm was multiexponential with time constants of 0.17, 0.8 and 7.9 ns (Fig. 4 and Table 1). The first value is attributed to geminate quenching. The second component corresponds well to the lifetime of 6′-**Me**-5,5-**Cpr-OxyL**

(0.9 ns, compare with the data in Table 1). At pH 10 the decay recorded at 550 nm was monoexponential with time constant ~8 ns. This result shows that the keto tautomer is not present in basic solution, and the spectra recorded under such conditions correspond to emission from the phenol-enolate-**OxyLH**$^-$.

Table 1. Time resolved and fluorescence quantum yield fluorescence data for firefly oxyluciferin and its derivatives (Chart 2) in aqueous solutions (the constants for **$OxyLH_2$** obtained by using the global analysis method for all the decay are highlighted in boldface font)

Compound	Neutral emission				Anionic emission					Φ_{Fl}
	pH	λ_{ex} / nm	λ_{em} / nm	τ / ns	pH	λ_{ex} / nm	λ_{em} / nm	τ / ns (%)		
4,6′-**DMeOxyL**	5–11	370	450	3.10	-					0.49
4-**MeOxyLH**	5	370	450	0.24[a]	5	370	560	0.21[b] 1.47 (11) 4.86 (89)		0.32
					10	430	560	4.88		0.47
6′-**Me**-5,5-**Cpr-OxyL**	5–9	390	525	0.93	-					0.11
5,5-**Cpr-OxyLH**	5	390	525	< 0.05[a]	5	390	640	0.16 (25) 0.61 (75)		0.18
					10	520	640	0.63		0.26
6′-**MeOxyLH**	5	370	450	< 0.05[a]	5	370	550	0.17 (42) 0.78 (32) 7.88 (26)		0.18
					10	430	550	7.97		0.35
$OxyLH_2$	5	370	450	< 0.05[a]	5	370	550	0.16 (52) 1.04 (8) 7.63 (40)	**0.17 (50)** **0.48 (7)** **7.82 (43)**	0.15
						370	640	0.16 (12) 0.56 (80) 7.28 (8)	**0.17 (41)** **0.48 (49)** **7.82 (10)**	
					7.6	430	550	0.17 (32) 0.53 (19) 3.95 (6) 7.68 (43)	**0.17 (17)** **0.48 (7)** **5.80 (19)** **7.82 (55)**	0.35
						510	640	0.41	**0.17 (2)** **0.48 (98)**	
					10	430	540	5.91	**5.80**	0.50

[a]Short component of non-exponential decay.
[b]Average time constant of the growing part.

3.4. Emission spectra of oxyluciferin (**OxyLH$_2$**)

The presence of five chemical forms strongly complicates the accurate spectral characterization of the pH-dependent emission of the real emitter (**OxyLH$_2$**), which also is the most intricate part of the analysis. To decipher the individual contributions, the fluorescence spectra of **OxyLH$_2$** were recorded at three different excitation wavelengths, UV excitation at 370 nm ,and visible excitation at 430 and 510 nm (Fig. 5). The selective photoexcitation greatly facilitated the interpretation of the spectra. The relative absorption intensities of the six chemical forms of **OxyLH$_2$** at selected pH are listed in Fig. 2.

Excitation at 370 nm. In acidic conditions (pH < 8), the dominant species excited at 370 nm are phenol-enol-**OxyLH$_2$** and phenol-keto-**OxyLH$_2$** (Fig. 2b and 2c). Assuming strong photoacidity in the excited state for enol group for phenol-enol form (pKa* is higher for enol than for phenol comparing results obtained for 6'MeOxyLH and 4-MeOxyLH, Table 2) and for phenol group for phenol-keto form, we can conclude that the first species should be deprotonated to phenol-enolate-**OxyLH**$^-$ whereas the second one to phenolate-keto-**OxyLH**$^-$. The efficient ESPT from the enol group is clearly visible in the time-resolved curve recorded at wavelength corresponding to the phenol-enol-**OxyLH$_2$** form (450 nm). The recorded decay indicates that the emission from the neutral form is strongly quenched and the proton transfer time constant is <50 ps (instrument response function) (Fig. 5b, Table 1). Erez et al. evaluated this value to 45 ps.[49] Taking into account the possible deprotonation of the phenol group, the fluorescence spectrum measured under such conditions should contain contributions from both species. In line with our expectations, a dominant contribution comes from the phenol-enolate-**OxyLH**$^-$ form (555 nm) because of its higher abundance and higher fluorescence quantum yield relative to phenolate-keto-**OxyLH**$^-$ (637 nm). Moreover, the contribution of this last species is clearly seen from the long wavelength tail of the recorded spectrum that extends beyond 600 nm (compare with the emission of 6′-**MeOxyLH** in Fig. 3e).

In addition to geminate recombination, at pH 5 the fluorescence decay recorded at 640 nm clearly shows two species with fluorescence time constants ~0.5 ns and ~7.3 ns. The former value is fully in line with the lifetime of the phenolate-keto-**OxyLH**$^-$ form determined by consideration of 5,5-**Cpr-OxyLH** (see section 3.3) whereas the latter is in good agreement with the fluorescence lifetime of phenol-enolate-**OxyLH**$^-$ (7.9 ns; Table 1) determined for 6′-**MeOxyLH**. By increase of pH, the contribution from the keto tautomer becomes marginal and the most abundant species are phenol-enolate-**OxyLH**$^-$ and **OxyL**$^{2-}$ (Fig. 2d and 2e). As a result, the observed emission spectra are slightly blue-shifted and are attributed to a mixture of monoanionic and dianionic form. The emission of the dianion becomes dominant for pH > 9 due to negligible concentration of other species in the ground state (Fig. 2f and 2g). Therefore, the spectrum recorded at pH = 11 with maximum at 539 nm can be assigned to **OxyL**$^{2-}$. This emission is blue-shifted compared to that of the mono-deprotonated form (phenol-enolate-**OxyLH**$^-$) and also has a shorter lifetime, ~5.9 ns (Table 1).

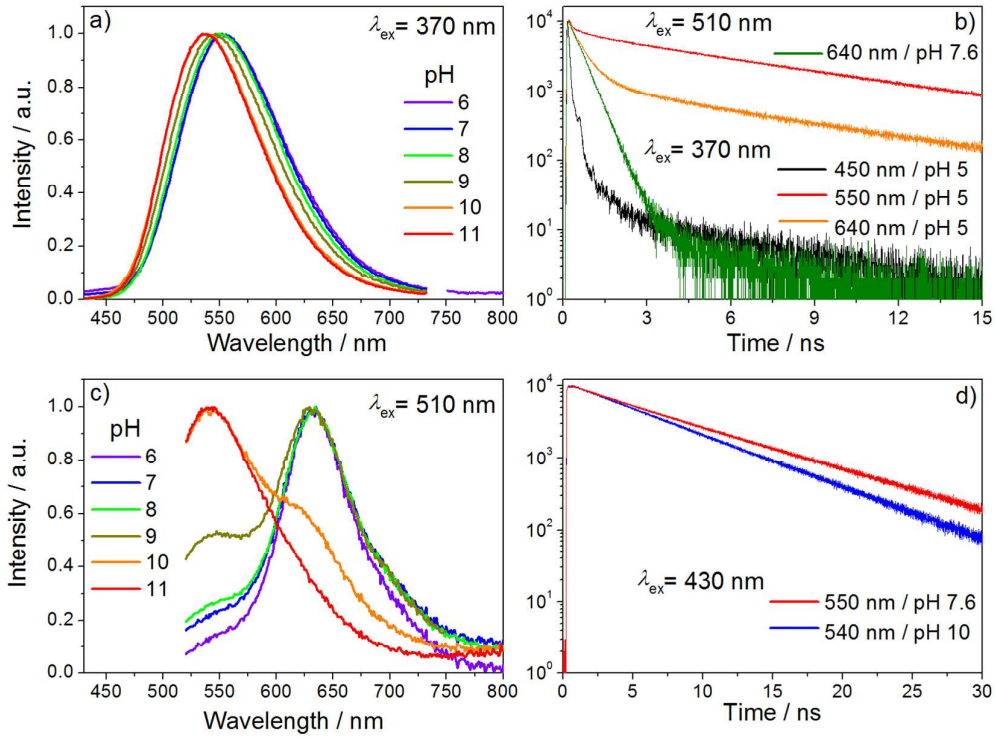

Figure 5. Normalized emission spectra of firefly oxyluciferin in aqueous solution at different pH and excitation wavelengths.

Excitation with visible light. Photoexcitation at lower energy leads to different photoluminescence pathways. In acidic solutions (pH 6 and 7) after 510 nm excitation the major absorbing species is the phenolate-keto-**OxyLH**$^-$ form (SI Fig. S7). Thus, the emission spectrum after 510 nm excitation is dominated by the phenolate-keto-**OxyLH**$^-$ form and features a band at 634 nm, which is slightly blue-shifted when compared to the 637 nm band of 5,5-**Cpr-OxyLH** in basic solution. The fluorescence decay at 640 nm is nearly monoexponential with a lifetime 0.4 ns (Fig. 5b, Table 1), indicating that the phenolate-keto-**OxyLH**$^-$ is the dominant species. At pH 8 and 9, a shoulder around 540 nm appears from **OxyL**$^{2-}$, in line with a pH-dependent increasing abundance of this species due to deprotonation of phenol-enolate-**OxyLH**$^-$ in the ground state. The emission decay at pH 7.6 after excitation at 430 nm detected at 550 nm shows a mixture of all species (Fig. 5d, Table 1) and by comparison with excitation at 510 nm, phenolate-keto (0.53 ns), **OxyL**$^{2-}$ (3.95 ns) and phenol-enolate-**OxyLH**$^-$ (7.68 ns). At pH 10, the intensity of the red band decreases considerably in favor of the green emission from **OxyL**$^{2-}$ (~540 nm) which becomes dominant at pH 11 with a lifetime of 5.91 ns.

The above analysis provides arguments for assigning the emission spectra of the individual chemical forms of firefly **OxyLH$_2$**, plotted in Fig. 6. Interestingly, the order of emission energies does not reflect exactly the order of the absorption energies (Table 2). The order of emission energies is phenol-enol-**OxyLH$_2$** (445 nm) > phenol-keto-**OxyLH$_2$** (525 nm) > phenolate-enolate-**OxyL**$^{2-}$ (539 nm) > phenol-enolate-**OxyLH**$^-$ (555 nm) > phenolate-enol-**OxyLH**$^-$ (560 nm) > phenolate-keto-**OxyLH**$^-$ (634 nm). Furthermore, for **OxyLH$_2$** the decay luminescence analysis shows that in excited state only three species (phenol-enolate, phenolate-keto and phenolate-enolate) are observed with one decay for geminate

recombination (0.17 ns) without any ESPT growing signal. This is in line with the results that the enol group in the phenol-enol form (phenol group has higher pK_a*, Table 2) and the phenol group in the phenol-keto form are strong photoacids. Accordingly, in addition to single wavelength lifetime analysis, a global decay analysis with four time constants was performed, one for each species and one for geminate recombination (Table 1) to arrive at more precise values for the phenol-enolate (7.82 ns), phenolate-keto (0.48 ns) and phenolate-enolate (5.80 ns) forms. At different excitation wavelengths and pH range, no growing signals were found in water contrary to time resolved spectra in toluene[47] which were indicative of isomerization or ionization from the phenolate-keto form or the phenol-enolate form to the phenolate-enolate form. This is in agreement with the order of emission energies of the phenolate-keto and phenol-enolate forms (adding to that mono-ionic species were reported to be more stable in the ground state than di-anionic species[37]) which seem to prevent conversion in the first excited state to phenolate-enolate form because they are at lower energy.

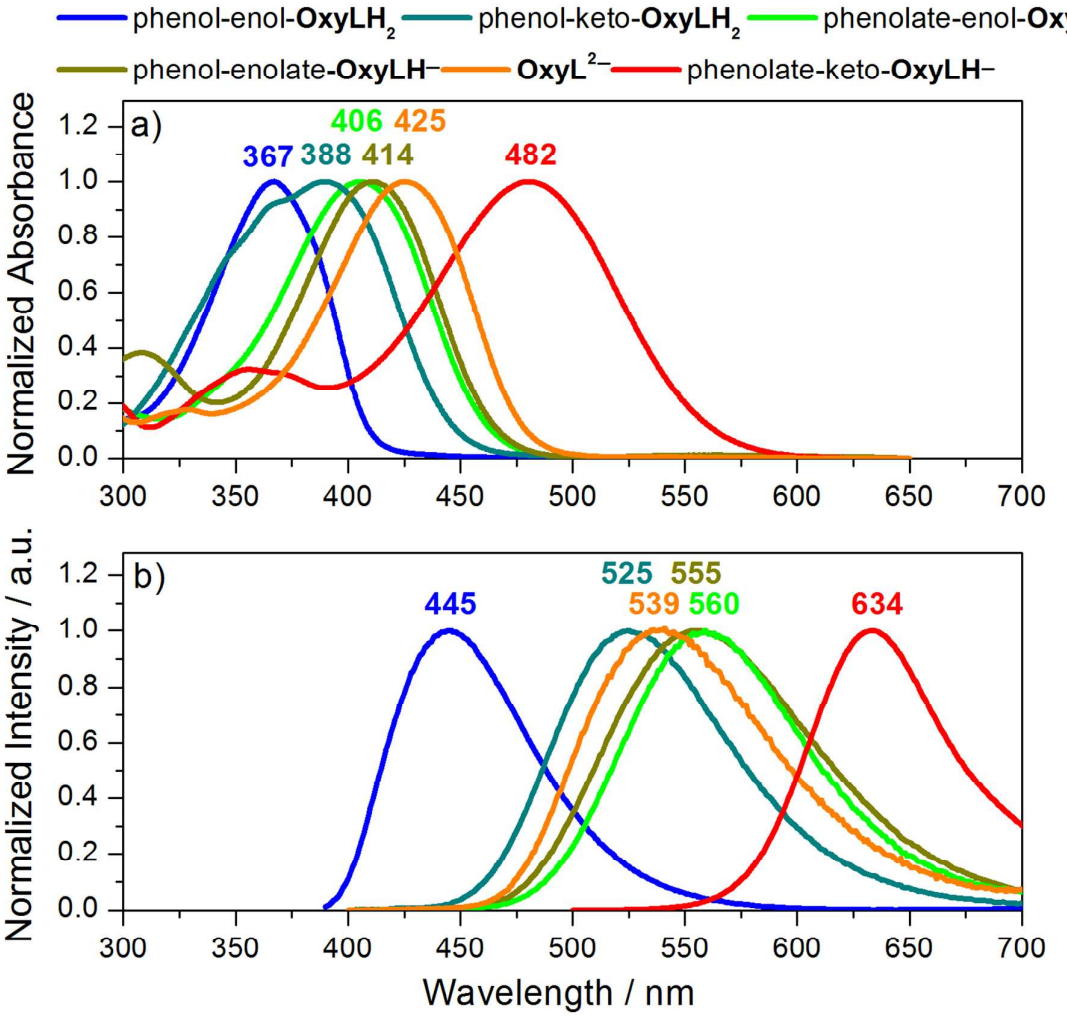

Figure 6. Absorption (top panel) and emission (bottom panel) spectra of individual chemical forms of firefly oxyluciferin based on the multivariate curve resolution–alternating least squares (MCR-ALS) procedure.

3.5. Equilibria and photodynamics in the excited state

Having determined the emission energies of all model compounds in their neutral and (wherever possible) anionic forms, the values for the estimated excited-state equilibrium constants (see section 3.1) can be corrected and refined. The pK_a* values recalculated by using the Förster cycle theory and the intersection points of the mutually normalized absorption and emission spectra of the conjugated acid-base pairs are presented in Table 2. Information about the excited-state equilibrium constants can also be derived from fitting nonexponential fluorescence decays of a conjugated acid to the numerical solution of the Debye-Smoluchowski equation. This method, known as the spherically symmetric diffusion problem (SSDP) approach, was recently successfully applied to various photoacids.[59]

The fluorescence decay at the wavelength corresponding to the neutral emitter band displays typically a bimodal character. The short decay component corresponds to emission from the neutral emitter quenched by ESPT (with rate constant k_{PT}) whereas the long tail is attributed to reversible geminate recombination process (k_r) (SI Fig. S6). Such nonexponential decay is clearly visible in the emission from 4-**MeOxyLH** recorded at 450 nm (Fig. 4a). The fitting procedure employed by using the SSDP software of Krissnel and Agmon[59] provided the rate constants of the proton transfer, $k_{PT} = 4.1 \times 10^9$ s^{-1}, and geminate recombination in the excited state, $k_r = 17 \times 10^9$ Å s^{-1}. The ratio k_{PT}/k_r[57] gives pK_a* = 2.0, in reasonable agreement with the value obtained by Förster cycle analysis. Unfortunately, the emission decays of the non-dissociated forms of the other compounds are nearly as short as our instrumental response (~50 ps) and the SSDP approach could not be applied.

In contrast to the reversible recombination, the irreversible process takes the molecule to the ground state with rate constant k_q (SI Fig. S6). This process is characterized by the presence of a short component in the fluorescence decay of anionic species in acidic conditions. This component is absent in basic solutions because the molecule is deprotonated before excitation (Fig. 4b, Table 1). Interestingly, the relative contribution of this short component throughout the decay depends on the functional group of the photoacid. 4-**MeOxyLH** exhibits a time constant ~1.5 ns with relative amplitude of 11% whereas 6′-**MeOxyLH** has a component of 0.17 ns with an amplitude of 42%. This result indicates that the irreversible geminate proton quenching is significantly more effective for the enol group. **OxyLH$_2$** has the highest contribution from the short decay component (52%) because the quenching takes place at both deprotonation sites.

Table 2. Spectroscopic parameters and equilibrium constants for firefly oxyluciferin and its analogues in aqueous solutions

Compound	λ_{abs} / nm		pK_a	λ_{em} / nm		pK_a*
	neutral	anion		neutral	anion	
4,6′-**DMeOxyL**	367	-	-	445	-	-
4-**MeOxyLH**	367	406	8.7	~450	560	0.9 ± 0.3
6′-**MeOxyLH**	371	414	7.3	~450	555	–0.3 ± 0.3
6′-**Me**-5,5-**Cpr-OxyL**	388	-	-	525	-	-
5,5-**Cpr-OxyLH**	388	482	7.8	n.d.	637	–1.0 ± 0.5
OxyLH$_2$	371	414[a] 425[b]	7.1[d] 9.0[e]	~450	539[b] 555[a] 634[c]	–0.9 ± 0.5[f] –0.5 ± 0.3[d] 1.2 ± 0.3[g] 7.5 ± 0.3[e]

[a]Phenol-enolate-**OxyLH**$^-$, [b]**OxyL**$^{2-}$, [c]Phenolate-keto-**OxyLH**$^-$, [d]Phenol-enol/phenol-enolate, [e]Phenol-enolate/phenolate-enolate, [f]Phenol-keto/phenolate-keto, [g]Phenol-enol/phenolate-enol, (n.d. – not detectable).

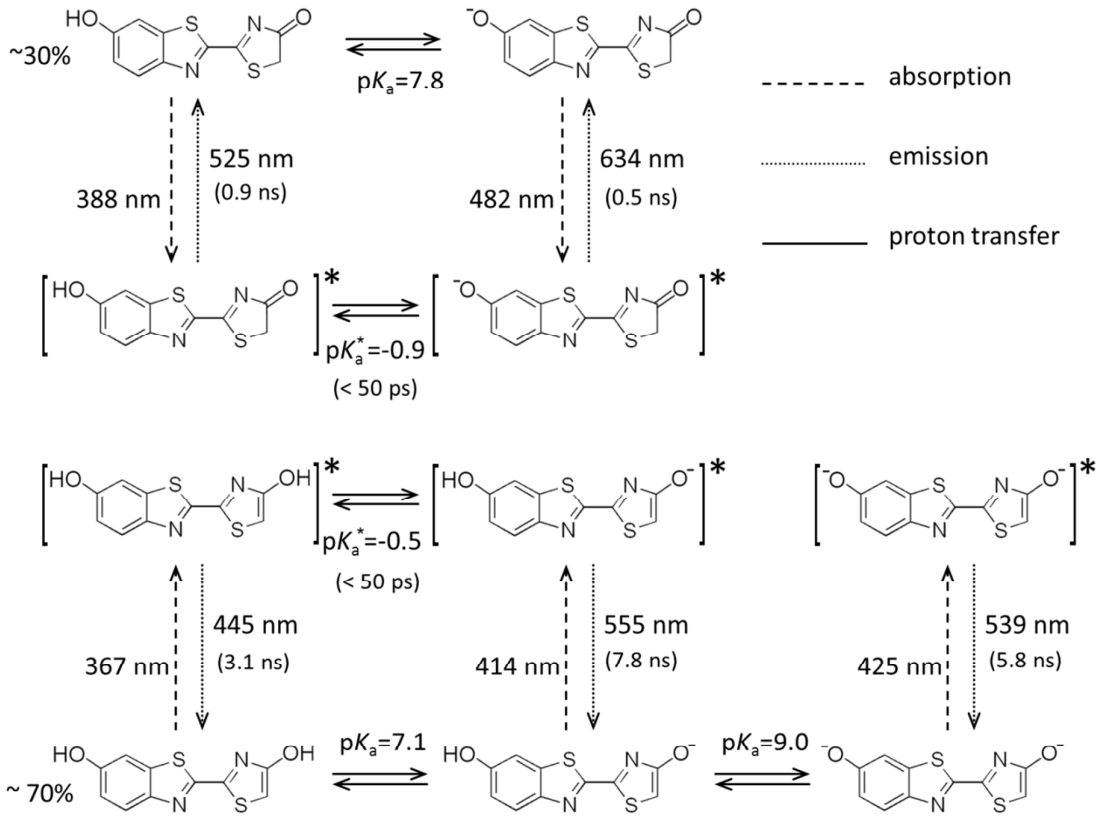

Scheme 2. Photoluminescence pathways of oxyluciferin in aqueous solution.

5. Conclusions

A combination of model compounds with thorough study of the pH-dependent steady-state and time-resolved fluorescence spectra revealed, for the first time, the emission spectra and luminescence lifetimes for all tautomeric forms and protonation states of firefly oxyluciferin in TRIS-buffered aqueous solutions. Using the Förster cycle approach, the excited-state equilibrium constants were also calculated. The most important conclusions from this study are:

(1) We found that contrary to previous conclusions[42] for the blue emission from the neutral phenol-keto isomer in non-aqueous solutions, a keto-oxyluciferin analogue (a cyclopropyl derivative) of this species is a green emitter (525 nm) in aqueous solution;

(2) We confirmed earlier conclusions[47] that ESPT from the enol group of the phenol-enol form is more favorable in the excited state than ESPT from the phenol group;

(3) The phenol-keto form is the strongest photoacid among the isomers;

(4) The phenolate-keto ion has the lowest emission energy (634 nm);

(5) The order of emission energies of the chemical forms of oxyluciferin and global analysis of the fluorescence decay indicates that some processes in the first excited state are not likely

to take place in strongly polar environment with strong hydrogen bonding potential, such as water. In particular, a second deprotonation at the phenol group after the enol deprotonation (i.e., deprotonation of the phenol-enolate) is not likely to occur in the excited state. Moreover, the keto-enol tautomerism reaction, observed previously in toluene in presence of a strong base,[47] is not favorable in water.

Finally by combining these data with our previous results as well as with the equilibrium constants determined in this work we can propose Scheme 2 for the complete photoluminescence cycle of **$OxyLH_2$** in a wide pH range in buffered aqueous solution. These results could be useful to gain better insight into the firefly bioluminescence. Indeed although these results do not directly apply to the luciferase where the active site is considered to be of low polarity, they provide support to the hypothesis that the excited-state potential energy surface and the related dynamics are affected by the environment of the active site.

Supporting Information. Stability, absorption, emission and time resolved fluorescence decays data for oxyluciferin and its analogues. This material is available free of charge via the Internet at http://pubs.acs.org.

Corresponding Authors
*Emails: pascal.didier@unistra.fr (P.D.), michel.sliwa@univ-lille1.fr (M.S.), pance.naumov@nyu.edu (P.N.)

Author Contributions
¶ These authors contributed equally to this study.
The manuscript was written through contributions of all authors. All authors have given approval to the final version of the manuscript.

Acknowledgments
This work was financially supported by the Human Frontier Science Program (project RGY0081/2011, "Excited-State Structure of the Emitter and Color-Tuning Mechanism of the Firefly Bioluminescence"). We thank also financial support from PICS CNRS-FWO Fund and New York University Abu Dhabi. Authors are thankful to Gilles Ulrich UMR 7515-ECPM-CNRS for providing facilities to measure absolute quantum yield of reference derivatives.

References

(1) Shimomura, O. *Bioluminescence: Chemical Principles and Methods*; World Scientific: Singapore, 2012.
(2) McCapra, F. Chemical mechanisms in bioluminescence. *Acc. Chem. Res.* **1976**, *9*, 201-208.
(3) Branchini, B. R.; Southworth, T. L.; Murtiashaw, M. H.; Magya, R. A.; Gonzalez, S. A.; Ruggiero, M. C.; Stroh, J. G. An Alternative Mechanism of Bioluminescence Color Determination in Firefly Luciferase. *Biochemistry* **2004**, *43*, 7255-7262.
(4) Suzuki, N.; Goto, T. Studies on Firefly Bioluminescence .3. Synthesis of 4-Thiazolone Derivatives Related to Firefly Oxyluciferin. *Agric. Biol. Chem.* **1972**, *36*, 2213-2221.
(5) White, E. H.; Rapaport, E.; Seliger, H. H.; Hopkins, T. A. The chemi- and bioluminescence of firefly luciferin: An efficient chemical production of electronically excited states. *Bioorg. Chem.* **1971**, *1*, 92-122.

(6) Ando, Y.; Niwa, K.; Yamada, N.; Enomot, T.; Irie, T.; Kubota, H.; Ohmiya, Y.; Akiyama, H. Firefly bioluminescence quantum yield and colour change by pH-sensitive green emission. *Nat. Photonics* **2008**, *2*, 44-47.
(7) Greer, L. F.; Szalay, A. A. Imaging of light emission from the expression of luciferases in living cells and organisms: a review. *Luminescence* **2002**, *17*, 43-74.
(8) Griffiths, M. W. The role of ATP bioluminescence in the food industry. *Food Technol.* **1996**, *50*, 62-73.
(9) Kricka, L. J. Application of bioluminescence and chemiluminescence in biomedical sciences. *Methods Enzymol.* **2000**, *305*, 333-345.
(10) Ohkuma, H.; Abe, K.; Kosaka, Y.; Maeda, M. Detection of luciferase having two kinds of luminescent colour based on optical filter procedure: application to an enzyme immunoassay. *Luminescence* **2000**, *15*, 21-27.
(11) Shinde, R.; Perkins, J.; Contag, C. H. Luciferin derivatives for enhanced in vitro and in vivo bioluminescence assays. *Biochemistry* **2006**, *45*, 11103-11112.
(12) Sun, Y.-Q.; Liu, J.; Wang, P.; Zhang, J.; Guo, W. D-Luciferin Analogues: a Multicolor Toolbox for Bioluminescence Imaging. *Angew. Chem., Int. Ed.* **2012**, *51*, 8428-8430.
(13) Ugarova, N. N. Interaction of firefly luciferase with substrates and their analogs: a study using fluorescence spectroscopy methods. *Photochem. Photobiol. Sci.* **2008**, *7*, 218-227.
(14) Ugarova, N. N.; Brovko, L. Y. Protein structure and bioluminescent spectra for firefly bioluminescence. *Luminescence* **2002**, *17*, 321-330.
(15) Hosseinkhani, S. Molecular enigma of multicolor bioluminescence of firefly luciferase. *Cell. Mol. Life Sci.* **2011**, *68*, 1167-1182.
(16) Wang, Y.; Hayamizu, Y.; Akiyama, H. Spectroscopic Study of Firefly Oxyluciferin in an Enzymatic Environment on the Basis of Stability Monitoring. *J. Phys. Chem. B* **2014**, *118*, 2070-2076.
(17) Branchini, B. R.; Murtiashaw, M. H.; Magyar, R. A.; Portier, N. C.; Ruggiero, M. C.; Stroh, J. G. Yellow-Green and Red Firefly Bioluminescence from 5,5-Dimethyloxyluciferin. *J. Am. Chem. Soc.* **2002**, *124*, 2112-2113.
(18) Branchini, B. R.; Rosenberg, J. C.; Ablamsky, D. M.; Taylor, K. P.; Southworth, T. L.; Linder, S. J. Sequential bioluminescence resonance energy transfer–fluorescence resonance energy transfer-based ratiometric protease assays with fusion proteins of firefly luciferase and red fluorescent protein. *Anal. Biochem.* **2011**, *414*, 239-245.
(19) Gandelman, O. A.; Brovko, L. Y.; Chikishev, A. Y.; Shkurinov, A. P.; Ugarova, N. N. Investigation of the interaction between firefly luciferase and oxyluciferin or its analogues by steady state and subnanosecond time-resolved fluorescence. *J. Photochem. Photobiol. B* **1994**, *22*, 203-209.
(20) Gandelman, O. A.; Brovko, L. Y.; Ugarova, N. N.; Shchegolev, A. A. The Bioluminescent System of Fireflies - Investigation of the Interaction of the Reaction-Product, Oxyluciferin, and its Analogs with Luciferase by Methods of Fluorescence Spectroscopy. *Biochemistry-Moscow* **1990**, *55*, 785-789.
(21) Min, K.-L.; Steghens, J.-P. The Emitting Species Dissociated from the Enzyme Can Emit the Light in Photinus pyralis Luciferase System. *Biochem. Biophys. Res. Commun.* **1999**, *265*, 273-278.
(22) Nakatsu, T.; Ichiyama, S.; Hiratake, J.; Saldanha, A.; Kobashi, N.; Sakata, K.; Kato, H. Structural basis for the spectral difference in luciferase bioluminescence. *Nature* **2006**, *440*, 372-376.
(23) Niwa, K.; Ichino, Y.; Kumata, S.; Nakajima, Y.; Hiraishi, Y.; Kato, D.-i.; Viviani, V. R.; Ohmiya, Y. Quantum Yields and Kinetics of the Firefly Bioluminescence Reaction of Beetle Luciferases. *Photochem. Photobiol.* **2010**, *86*, 1046-1049.

(24) Ugarova, N. N.; Maloshenok, L. G.; Uporov, I. V.; Koksharov, M. I. Bioluminescence Spectra of Native and Mutant Firefly Luciferases as a Function of pH. *Biochemistry-Moscow* **2005**, *70*, 1262-1267.
(25) Viviani, V. R.; Arnoldi, F. G. C.; Neto, A. J. S.; Oehlmeyer, T. L.; Bechara, E. J. H.; Ohmiya, Y. The structural origin and biological function of pH-sensitivity in firefly luciferases. *Photochem. Photobiol. Sci.* **2008**, *7*, 159-169.
(26) Wang, Y.; Akiyama, H.; Terakado, K.; Nakatsu, T. Impact of Site-Directed Mutant Luciferase on Quantitative Green and Orange/Red Emission Intensities in Firefly Bioluminescence. *Sci. Rep.* **2013**, *3*.
(27) Yanagisawa, Y.; Kageyama, T.; Wada, N.; Tanaka, M.; Ohno, S.-y. Time Courses and Time-Resolved Spectra of Firefly Bioluminescence Initiated by Two Methods of ATP Injection and Photolysis of Caged ATP. *Photochem. Photobiol.* **2013**, *89*, 1490-1496.
(28) Anselmi, M.; Marocchi, S.; Aschi, M.; Amadei, A. Theoretical modeling of the spectroscopic absorption properties of luciferin and oxyluciferin: A critical comparison with recent experimental studies. *Chem. Phys.* **2012**, *392*, 205-214.
(29) Chen, S.-F.; Liu, Y.-J.; Navizet, I.; Ferré, N.; Fang, W.-H.; Lindh, R. Systematic Theoretical Investigation on the Light Emitter of Firefly. *J. Chem. Theory Comput.* **2011**, *7*, 798-803.
(30) Pinto da Silva, L.; Esteves da Silva, J. C. G. Computational Studies of the Luciferase Light-Emitting Product: Oxyluciferin. *J. Chem. Theory Comput.* **2011**, *7*, 809-817.
(31) Hiyama, M.; Akiyama, H.; Wang, Y.; Koga, N. Theoretical study for absorption spectra of oxyluciferin in aqueous solutions. *Chem. Phys. Lett.* **2013**, *577*, 121-126.
(32) Kim, H. W.; Rhee, Y. M. On the pH Dependent Behavior of the Firefly Bioluminescence: Protein Dynamics and Water Content in the Active Pocket. *J. Phys. Chem. B* **2013**, *117*, 7260-7269.
(33) Li, Z.-w.; Ren, A.-m.; Guo, J.-f.; Yang, T.; Goddard, J. D.; Feng, J.-k. Color-Tuning Mechanism in Firefly Luminescence: Theoretical Studies on Fluorescence of Oxyluciferin in Aqueous Solution Using Time Dependent Density Functional Theory. *J. Phys. Chem. A* **2008**, *112*, 9796-9800.
(34) Nakatani, N.; Hasegawa, J.-Y.; Nakatsuji, H. Red Light in Chemiluminescence and Yellow-Green Light in Bioluminescence: Color-Tuning Mechanism of Firefly, Photinus pyralis, Studied by the Symmetry-Adapted Cluster−Configuration Interaction Method. *J. Am. Chem. Soc.* **2007**, *129*, 8756-8765.
(35) Navizet, I.; Liu, Y.-J.; Ferré, N.; Xiao, H.-Y.; Fang, W.-H.; Lindh, R. Color-Tuning Mechanism of Firefly Investigated by Multi-Configurational Perturbation Method. *J. Am. Chem. Soc.* **2010**, *132*, 706-712.
(36) Navizet, I.; Roca-Sanjuán, D.; Yue, L.; Liu, Y.-J.; Ferré, N.; Lindh, R. Are the Bio- and Chemiluminescence States of the Firefly Oxyluciferin the Same as the Fluorescence State? *Photochem. Photobiol.* **2013**, *89*, 319-325.
(37) Orlova, G.; Goddard, J. D.; Brovko, L. Y. Theoretical Study of the Amazing Firefly Bioluminescence: The Formation and Structures of the Light Emitters. *J. Am. Chem. Soc.* **2003**, *125*, 6962-6971.
(38) Pinto da Silva, L.; Esteves da Silva, J. C. G. Computational Investigation of the Effect of pH on the Color of Firefly Bioluminescence by DFT. *ChemPhysChem* **2011**, *12*, 951-960.
(39) Ren, A.-M.; Guo, J.-F.; Feng, J.-K.; Zou, L.-Y.; Li, Z.-W.; Goddard, J. D. TDDFT Study of the Electronic Structure, Absorption and Emission Spectra of the Light Emitters of the Amazing Firefly Bioluminescence and Solvation Effects on the Spectra. *Chin. J. Chem.* **2008**, *26*, 55-64.

(40) Song, C.-I.; Rhee, Y. M. Dynamics on the Electronically Excited State Surface of the Bioluminescent Firefly Luciferase–Oxyluciferin System. *J. Am. Chem. Soc.* **2011**, *133*, 12040-12049.
(41) Naumov, P.; Kochunnoonny, M. Spectral−Structural Effects of the Keto−Enol−Enolate and Phenol−Phenolate Equilibria of Oxyluciferin. *J. Am. Chem. Soc.* **2010**, *132*, 11566-11579.
(42) Naumov, P.; Ozawa, Y.; Ohkubo, K.; Fukuzumi, S. Structure and Spectroscopy of Oxyluciferin, the Light Emitter of the Firefly Bioluminescence. *J. Am. Chem. Soc.* **2009**, *131*, 11590-11605.
(43) Rebarz, M.; Kukovec, B. M.; Maltsev, O. V.; Ruckebusch, C.; Hintermann, L.; Naumov, P.; Sliwa, M. Deciphering the protonation and tautomeric equilibria of firefly oxyluciferin by molecular engineering and multivariate curve resolution. *Chem. Sci.* **2013**, *4*, 3803-3809.
(44) Maltsev, O. V.; Nath, N. K.; Naumov, P.; Hintermann, L. Why is firefly oxyluciferin a notoriously labile substance? *Angew. Chem., Int. Ed.* **2014**, *53*, 847–850.
(45) Hirano, T.; Hasumi, Y.; Ohtsuka, K.; Maki, S.; Niwa, H.; Yamaji, M.; Hashizume, D. Spectroscopic Studies of the Light-Color Modulation Mechanism of Firefly (Beetle) Bioluminescence. *J. Am. Chem. Soc.* **2009**, *131*, 2385-2396.
(46) Wang, Y.; Kubota, H.; Yamada, N.; Irie, T.; Akiyama, H. Quantum Yields and Quantitative Spectra of Firefly Bioluminescence with Various Bivalent Metal Ions. *Photochem. Photobiol.* **2011**, *87*, 846-852.
(47) Solntsev, K. M.; Laptenok, S. P.; Naumov, P. Photoinduced Dynamics of Oxyluciferin Analogues: Unusual Enol "Super"photoacidity and Evidence for Keto–Enol Isomerization. *J. Am. Chem. Soc.* **2012**, *134*, 16452-16455.
(48) Sundlov, J. A.; Fontaine, D. M.; Southworth, T. L.; Branchini, B. R.; Gulick, A. M. Crystal Structure of Firefly Luciferase in a Second Catalytic Conformation Supports a Domain Alternation Mechanism. *Biochemistry* **2012**, *51*, 6493-6495.
(49) Erez, Y.; Presiado, I.; Gepshtein, R.; Pinto da Silva, L.; Esteves da Silva, J. C. G.; Huppert, D. Comparative Study of the Photoprotolytic Reactions of d-Luciferin and Oxyluciferin. *J. Phys. Chem. A* **2012**, *116*, 7452-7461.
(50) Ando, Y.; Akiyama, H. pH-Dependent Fluorescence Spectra, Lifetimes, and Quantum Yields of Firefly-Luciferin Aqueous Solutions Studied by Selective-Excitation Fluorescence Spectroscopy. *Jpn. J. Appl. Phys.* **2010**, *49*.
(51) Hiyama, M.; Akiyama, H.; Mochizuki, T.; Yamada, K.; Koga, N. Analysis of Photoexcitation Energy Dependence in the Photoluminescence of Firefly Luciferin. *Photochem. Photobiol.* **2014**, *90*, 820-828.
(52) *Throughout this work unprimed locants refer to the thiazole/thiazolone part and primed locants to the benzothiazole part of oxyluciferin and its analogs.*
(53) Lakowicz, J. R. *Principles of Fluorescence Spectroscopy*; Springer: New York, 2006.
(54) White, E. H.; Roswell, D. F. Analogs and Derivatives of Firefly Oxyluciferin, the Light Emitter in Firefly Bioluminescence. *Photochem. Photobiol.* **1991**, *53*, 131-136.
(55) Leonteva, O. V.; Vlasova, T. N.; Ugarova, N. N. Dimethyl- and monomethyloxyluciferins as analogs of the product of the bioluminescence reaction catalyzed by firefly luciferase. *Biochemistry-Moscow* **2006**, *71*, 51-55.
(56) *Calculation was performed using the formula* $pK^{*}=pK+(E_{HA}-E_{A})/2.3RT$ *where pK is the value for the ground state, T is absolute temperature, R is the gas constant and* E_{HA} *and* E_{A} *are the energies of the protonated and dissociated form estimated from absorption maxima.*
(57) Solntsev, K. M.; Huppert, D.; Agmon, N. Photochemistry of "Super"-Photoacids. Solvent Effects. *J. Phys. Chem. A* **1999**, *103*, 6984-6997.

(58) Gandelman, O. A.; Brovko, L. Y.; Ugarova, N. N.; Chikishev, A. Y.; Shkurimov, A. P. Oxyluciferin fluorescence is a model of native bioluminescence in the firefly luciferin—luciferase system. *J. Photochem. Photobiol. B* **1993**, *19*, 187-191.
(59) Krissinel, E. B.; Agmon, N. Spherical symmetric diffusion problem. *J. Comput. Chem.* **1996**, *17*, 1085-1098.

Table of Contents